Nonlinear ionization waves

Tzihong Chiueh* and David M. T. Kuo
Physics Department and Center for Complex Systems, Institute of Astronomy, National Central University, Chung-Li, Taiwan
(Received 11 September 1997)

Spontaneously generated ionization wave patterns, which exhibit hyteresis, have been observed to exist in some narrow range of experimental conditions [J. B. Du, C. H. Chiang, and Lin I, Phys. Rev. E **54**, 1829 (1996)]. The present work reports a theoretical model for explaining these observations. Including the plasma ionization, losses, and collisions, the phenomenon can be interpreted as a reaction-diffusion problem. It has been found that there exists an internally generated order parameter, which plays an important role in governing the observed hysteresis. [S1063-651X(98)02004-2]

PACS number(s): 52.35.Lv, 47.54.+r, 52.90.+z

Plasma systems are known to contain many types of collective modes. Most familiar collective modes are excited in systems with little dissipation; the examples range from the high-frequency electron waves to the low-frequency hydromagnetic waves. Prompted by the advent of recent material and astrophysics research, the foci of many investigations in plasma physics, in the most recent decade, have been shifted to the studies of systems that are highly dissipative. Partially ionized plasmas are commonly found in many operation regimes of material processing [1]. Studies on the formation of the early solar system reveal that the dynamics of partially ionized dusty plasmas holds the key to the birth of meteorites and planets [2].

The presence of large dissipation and ample free-energy sources opens up a regime for these partially ionized plasmas in their excitations of collective motion [3]. Of particular interest is that, when excited, the dissipative structures associated with the collective behaviors appear rather robust and stable. Impressive examples include, among others, the dusty-plasma crystals [4,5,6] and solitary ionization waves [7,8]. These systems exhibit self-organized, ordered spatial patterns that emerge only after complicated mode competition and selection. Emergence of order has already been demonstrated in laboratories for the fluid, optical, and chemical systems [9–15]. Only recently, however, has such a phenomenon been systematically studied in a system that is as complicated and as uncontrollable as a plasma.

A recent work reports an experimental study of controllable, large-amplitude ionization waves in rf discharged plasmas [7]. Existence of ionization patterns in a partially ionized plasma is not new; one may often observe them in a damaged fluorescent lamp near the electrodes. However, this experiment enables manipulation of the spatial patterns by changing the experimental parameters and observation of the detailed evolution of the patterns. Among the interesting phenomena observed in the experiments, it is found that the patterns exhibit hysteresis in a controllable manner. The experimental system consists of two cylindrical electrodes, and the ionization patterns appear within a narrow annular dent on the inner electrode surface. The experiment operates at a pressure of about 500 mtorr, corresponding to 10^{16} neutral argon particles per cubic centimeter. With electrons at the 3-eV temperature, the ionization fraction is found to be about one part in 10^6. Both neutral atoms and ions are not in thermal equilibrium with the electrons and they are at room temperature. The thermal speed of argon particles is therefore about 5×10^4 cm/sec, giving the collisional time ν^{-1} among argon particles of about 2×10^{-7} sec, a rather short time scale compared to the ion transit time and indicative of a highly collisional plasma. On the other hand, the plasma is vigorously driven by an external rf source for ionization and energization. Thus, the system is indeed subject to high dissipation and is sustained by a large energy drive, characteristic of the driven-dissipative systems.

In the present work, we report a theoretical model attempting to address the nature of these ionization patterns in this driven-dissipative system. To begin the model construction, we first give an estimate of the system parameters. Subjected to severe ion-neutral collisions, the cool ions satisfy the momentum equation along the annulus (z):

$$m_i\left[\frac{\partial v_z}{\partial t}+\frac{\partial}{\partial z}\left(\frac{v_z^2}{2}\right)\right]=-e\,\frac{\partial\phi}{\partial z}-m_i\nu v_z, \tag{1}$$

where ϕ is the electric potential. One may balance the electric force with the ion frictional force to estimate the dynamical ion velocity. Typical potential drop is estimated to be about 10 V in the system, and the length scale to be about 1–2 cm for the wave patterns along z, yielding an electric field approximately 5–10 V/cm. It follows that the typical ion speed is about 10^5 cm/sec, corresponding to an ion kinetic energy of 0.1 eV, which is much smaller than the typical electric potential-energy scale of 10 eV. Thus, in the presence of the high ion-neutral collision rate, the ion inertial force [the left-hand side of Eq. (1)] is small compared to the electric force, and Eq. (1) can hence be rewritten as

$$\nu v=-\frac{e}{m_i}\frac{\partial\phi}{\partial z}. \tag{2}$$

On the other hand, the electrons are hot ($T_e\sim3$ eV) and light; the ratio of the frictional force to the electric force is smaller than that for the ions by a factor $\sqrt{m_eT_e/m_iT_i}\ll1$, and the electron frictional force can thus be ignored. In addition, since the electron dynamical velocity must be compa-

*Electronic address: chiueh@joule.phy.ncu.edu.tw

rable to that of ions 10^5 cm/sec (otherwise the electric current would be unreasonably large), it follows that the electron inertia force is also negligible. As a result, the electron pressure force $-T_e\partial n_e/\partial z$ must always balance the electric force $e\partial\phi/\partial z$, and it yields

$$n_e = n_0 e^{e\phi/T_e}, \tag{3}$$

where n_0 is an integration constant.

In fact, the ions within the annular dent are subject to severe loss of particles to the confining walls. We may estimate the rate of ion losses. The transverse ion velocity, at which the ions impinge into the confining walls, is estimated to be about 5×10^5 cm/sec, considerably larger than the ion velocity along z, and corresponding to an ion flow with the Mach number ($\equiv\sqrt{m_i v_\perp^2/T_e}$) equal to unity. (This requirement for the ion Mach number is essential for sustaining a plasma sheath near the confining walls [16].) Moreover, the transverse length scale (half width of the annular dent) is 1.5 mm, and the estimated ion-loss rate $\beta(\sim v_\perp/L_\perp)$ therefore amounts to about 3×10^6 sec^{-1}. This ion sink can thus be modeled as $-\beta n_i$. Another possible ion loss is through the three-body recombination of ions with electrons mediated by the presence of neutral particles. In this highly collisional regime, the dense neutral particles make almost every collision between ions and electrons a three-body process, much like collisions of two rocks in water in which the water molecules always participate in the collisions. The ion loss rate is therefore $(n_e\sigma v_{te})$, with the recombination cross section σ about 10^{-15} cm^2, the electron-density n_e about 10^{12} cm^{-3}, and the electron thermal speed v_{te} about 10^8 cm/sec. The ion-recombination loss rate is therefore 10^5 sec^{-1}, much smaller than the rate of ion loss to the wall (3×10^6 sec^{-1}) and, hence, can be ignored.

Meanwhile, replenishment of fresh ions is essential in maintaining the glow discharge. In the experiments the plasmas are discharged by the rf, where electrons are accelerated by the rf and ionize the neutral particles upon colliding with them. Therefore, the ion source must be proportional to the electron density n_e, the neutral density, and the rf power. The neutral particle density is much larger than the electron density, and thus the neutral density is essentially unchanged and uniform. We therefore model the ion source as αn_e. Since the ion density is comparable to the electron density, the replenishing rate α is expected to be of the same order as the loss rate β which makes the ion source just balance the ion sink.

With these considerations, the ion density, after an average over the cross section of the annular dent, satisfies

$$\frac{\partial N_i}{\partial t}+\frac{\partial}{\partial z}(N_i v)=\alpha N_e-\beta N_i. \tag{4}$$

Here, $N\equiv\int d\mathbf{x}_\perp n/(\pi l_\perp^2)$, the cross-section-averaged density, and $\pi l_\perp^2$ is the cross section of the annular dent.

To close the relations between v, N_e, N_i, and ϕ, we need to employ Poisson's equation to address the space charge:

$$\nabla^2\phi=-4\pi e(n_i-n_e). \tag{5}$$

The equation should be handled with care since this problem is not entirely a one-dimensional problem. The actual electric-field lines should usually not be along the annulus cavity but diverge away from the cavity into the plasma chamber and electrode. Thus, the electric interactions within the annular dent arise primarily from the multipole interactions and are therefore essentially short ranged if the typical length scale of charge distribution along the annulus is much greater than the transverse dimension of the annular dent. We may show this nature of short-range forces by the following considerations.

Consider a charged line with a certain pattern of charge distribution $\pi l_\perp^2 e\Delta N(z)$, where $\Delta N\equiv(N_i-N_e)$. Upon integrating Eq. (5) over the cross section of the line, taking a Fourier transform for z and assuming axisymmetry, we find that

$$\left(2\pi r\,\frac{d\phi_k}{dr}\right)\Bigg|_0^{l_\perp}-k^2\int_0^{l_\perp}2\pi r\,dr\;\phi_k=-4\pi^2 l_\perp^2 e\Delta N_k. \tag{6}$$

Since $l_\perp$ is a small length compared to the wavelength along the line k^{-1}, we may ignore the second term on the left provided that the potential ϕ_k is smooth and finite. Away from the charged line, we found that Eq. (5) has no source and becomes a Laplace equation. With the boundary condition that the electric field vanishes at infinity ($r\to\infty$), the solution to the Fourier-transformed (in z) Laplace equation is

$$\phi_k=cK_0(kr), \tag{7}$$

where K_0 is the modified Bessel function and c is a constant. Note that this solution is valid only within $l_\perp<r<\infty$, and can be used to determine the radial electric field $-d\phi_k/dr$ evaluated at the boundary $r=l_\perp$. Demanding that the charged line has no surface charge, it follows that the radial electric field must be continuous across the boundary, and the first term on the right-hand-side of Eq. (6) can therefore be determined. We thus solve for ϕ_k evaluated at $r=l_\perp$:

$$\phi_k=\left(\frac{-K_0(\epsilon)}{4\epsilon(dK_0(\epsilon)/d\epsilon)}\right)4\pi l_\perp^2 e\Delta N_k\equiv 4\pi c_0 l_\perp^2 e\Delta N_k, \tag{8}$$

where $\epsilon\equiv kl_\perp$ and c_0 is defined to be the quantity in the brace. When $\epsilon\ll1$, the modified Bessel's function $K_0(\epsilon)\to\ln(\epsilon)$ and, hence, $c_0\to-\ln(\epsilon)/4$, a positive definite quantity. Note that $-\ln(\epsilon)$ is very insensitive to ϵ and, hence, can be regarded as a constant with a value slightly above unity. In the experiment, the wavenumber k ranges from 1 to 2 cm^{-1} and $l_\perp\approx0.15$ cm, therefore, giving $0.15<\epsilon<0.3$ and justifying the small ϵ expansion. We may rewrite Eq. (8) as

$$\phi=(4\pi c_0 l_\perp^2 e)(N_i-N_e) \tag{9}$$

in the real-space representation. Equation (9) thus becomes the counterpart of Poisson's equation given in Eq. (5) for a line charge, where the nature of three-dimensional electric fields have been accounted for. The fact that the potential, instead of the Laplacian of the potential, becomes proportional to the line charge demonstrates the short-range nature of electric forces within the line.

The above example considers only the ideal case where the charged line is surrounded by a vaccum. In the real experiments, the charged annulus is surrounded by a rather complicated environment. Nonetheless, the effects of this complication can be incorporated into the positive coefficient c_0, which can only be determined by careful measurements of the electric fields by experiments, though one can assume a value of the same order as that estimated above.

Equations (2,3,4,9) can be combined to give a nonlinear reaction-diffusion equation:

$$(e^{\psi}+a)\frac{\partial\psi}{\partial\tau}-\frac{\partial}{\partial\xi}(e^{\psi}+a\psi)\frac{\partial\psi}{\partial\xi}=(1-\gamma)e^{\psi}-a\gamma\psi, \tag{10}$$

where $\psi\equiv e\phi/T_e$, $\tau\equiv\alpha t$, $\xi\equiv z\sqrt{m_i\nu\alpha/T_e}$, $\gamma\equiv\beta/\alpha$, and $a\equiv c_0^{-1}(\lambda_d/l_\perp)^2$. Here λ_d is the Debye length defined by the electron density N_0 in the background dark region, which is about a few times 10^8 cm^{-3} in the experiments and, hence, $\lambda_d\sim 0.1$ cm for the 3-eV electrons. With $\epsilon\sim 0.2$, one finds that $c_0=-\ln(\epsilon)/4\sim 0.4$ if the system is assumed to be an ideal line in vaccum described above. Given that $l_\perp\approx 0.15$ cm, it follows that $a\sim 1$.

At the *steady states*, we have $\partial/\partial\tau=0$ and Eq. (10) can be integrated once after multiplying both sides by $(e^{\psi}+\alpha\psi)(d\psi/d\xi)$. It yields

$$\tfrac{1}{2}\left(\frac{d\psi}{d\xi}\right)^2+U(\psi)=0, \tag{11}$$

where

$$U(\psi)\equiv\frac{1}{3(e^{\psi}+a\psi)^2}\left(-a^2\gamma\psi^3+3a(1-2\gamma)(\psi-1)e^{\psi}+\frac{3(1-\gamma)}{2}e^{2\psi}+E\right), \tag{12}$$

where E is the integration constant, a spontaneously generated ''order parameter'' that turns out to serve as an approximate indicator of the system energy.

To determine the viable solutions, it suffices to examine the structures of $U(\psi)$ as a function of the three parameters a, γ, and E. Any physical solution must have a finite range of ψ where $U(\psi)<0$. This requirement can only be fulfilled in some range of the two-parameter space (a,γ). Typically, the trend is such that when a decreases γ must approach unity from below. When γ assumes values larger than unity, corresponding to smaller ionization rates than the loss rates, *no* physical solution may exist.

Shown in Fig. 1 are the three typical $U(\psi)$'s in the neighborhood of the parameter regimes producing the observed nonlinear wave trains in experiments. These cases correspond to the parameters (a) $(a,\gamma,E)=(1,0.8,-2.225)$, (b) $(1,0.92,-0.5)$, and (c) $(1,0.92,-2.562)$. Figure 2 shows the respective solutions for $N_e/N_{\min}$ (dashed lines) and $N_i/N_{\min}$ (solid lines), where $N_{\min}$ is the minimum electron density of the wave pattern. Although the ion- and electron-density profiles are almost identical, the plasma is actually slightly nonneutral, biased against electrons, and exhibiting an overall positive plasma potential. This charge asymmetry results from the fact that ions are subject to severe neutral drags, whereas electrons are less so. Also note that at lower γ (higher neutral pressure), the density contrast of the ionized plasma is significantly reduced, due primarily to an increase in the background plasma density.

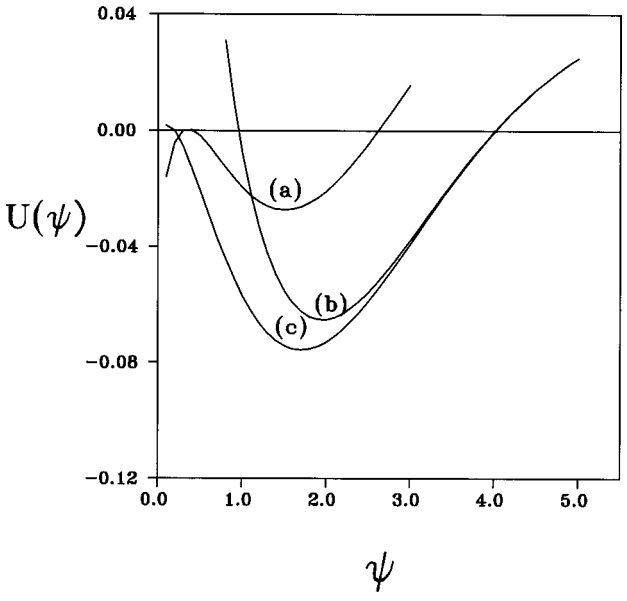

FIG. 1. Pseudo-potentials $U(\psi)$ that yield the corresponding plasma densities shown in Fig. 2. The three curves are for the dimensionless parameters (a,γ,E) are (a) $(1,0.8,-2.225)$, (b) $(1,0.92,-0.5)$, and (c) $(1,0.92,-2.562)$.

In the experiments [7], it has been found that as the neutral gas pressure increases, the mode number of the wave trains increases in a stepwise fashion, a fact simply reflecting

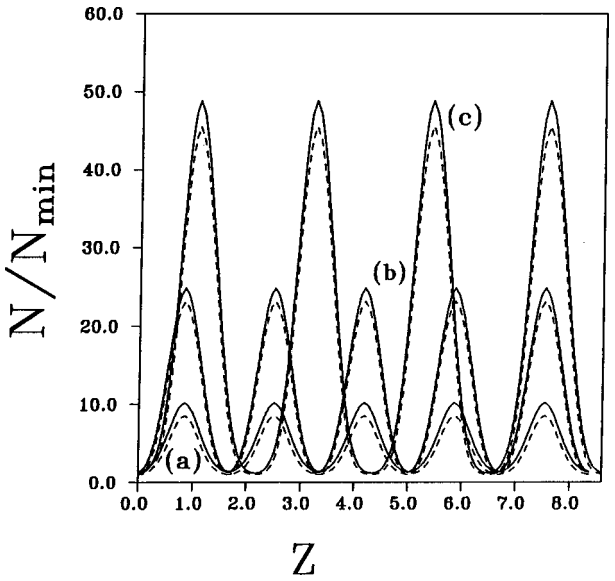

FIG. 2. Electron (dashed lines) and ion (solid lines) densities normalized to the minimum electron densities for the parameters given in Fig. 1. The length z (in cm) represents the actual experimental setup [7] for cases (a), (b), and (c) of Fig. 1, where the dimensionless parameter $\gamma=0.92$ corresponds approximately to 500 mtorr neutral pressure in the experiment and $\gamma=0.8$ corresponds to 600 mtorr.

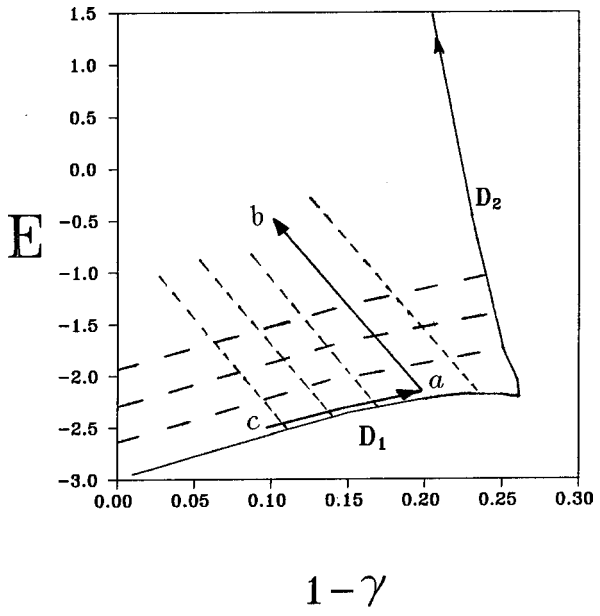

FIG. 3. The phase diagram in the (E,γ) space. The permissible region where the nonlinear ionization waves exist is bounded by the curves D_2, D_1 and the $\gamma=1$ axis. The actual trajectory observed in the experiment is, on the average, along the path from c, a to b, whose detailed solutions are given in Fig. 2. The schematic plots of the long- and short-dashed lines represents two families of curves, $G(E,\gamma)=C_a$ and $H(E,\gamma)=C_b$, respectively, along which the experimental trajectories are expected to follow.

the discrete nature of mode numbers around the annulus. The mode number increases from $m=8$ at a pressure of 500 mtorr to $m=11$ at 600 mtorr, where the diffusion length ($\propto \nu^{-1/2}$) decreases by a factor of 1.1 but the wavelength decreases by a factor of 1.4, indicating that a certain kind of dynamical mode selection is in operation. It has also been found in the experiments that the ionization waves exhibit hysteresis. The high-m mode ($m=11$) can survive as one reduces the neutral gas pressure after the pressure is initially increased. This high-m mode is a metastable mode and should have a higher energy than the low-m mode at the same pressure.

As the experiment rapidly quenches only a single parameter (the pressure of neutral argon which is inversely proportional to the parameter γ), one observes that the nonlinear waves assume the metastable states. To address the issue of hysteresis from the perspective of this theoretical model, it is essential to note that Eq. (10) in fact contains two independent parameters, γ and E, which permit the system to be at different states even when one of the two parameters assumes the same value. The parameter E is in fact an internally generated parameter, not externally controllable, and it arises in accordance with some internal dynamics of the system whereby the imprints of the past evolution are recorded. How the imprints can get recorded in E is beyond the scope of this work, which deals only with the steady states. Some hints can, nevertheless, be provided by the following considerations.

The range in the (γ,E) space, where the solutions exist, is indicated by the region in Fig. 3 that is bounded by D_2, D_1, and the $\gamma=1$ axis. The fact that the hysteresis follows a particular path in the permissible region must imply that the two parameters γ and E are dynamically related; that is, E can be expressed as a function $E(\gamma)$. Moreover, due to the presence of the hysteresis, $E(\gamma)$ should be a double-valued function. That is, there exist a stable branch of $E(\gamma)$ and a metastable branch of $E(\gamma)$. The two types of solutions in the (E,γ) space trace two families of lines. (In Fig. 3, we qualitatively sketch the anticipated two families of different dashed lines simply for the purpose of illustration.) The trajectory originally moves along a line in the stable family $G(\gamma,E)=C_a$ (long-dashed lines), and when the system is rapidly depressurized, it switches to the metastable family $H(\gamma,E)=C_b$ (short-dashed lines) on entering the hysteresis phase, where C_a and C_b are constants. The constants C_a and C_b may need to take discrete values; this issue will be discussed at the end of this paper. Although it is not yet understood what determines the functional forms of $G(\gamma,E)$ and $H(\gamma,E)$, with the aid of the only path in the published experimental data, we may nevertheless construct the trajectory of this path in our (γ,E) phase space, with the hope that when more experimental data become available, these functions can be fixed experimentally.

Among the stable family of lines $G(\gamma,E)=$const, when the plasma in the experiments is initially turned on, it always chooses to follow a particular path [from (c) to (a) in Fig. 3] as the system pressure is increased. This particular path lies near the bottom boundary of the permissible region in Fig. 3, indicative of a very stable path along which E assumes a value near that which is minimally allowable for a given neutral density, or γ. During the phase of increasing pressure, or decreasing γ [from (c) to (a)], we find it necessary to increase E in order for the mode number to increase as observed in the experiments. Figure 2 shows the comparison between the $m=8$ (c) and $m=11$ (a) modes at different neutral pressures. Since the changes of mode number must be discrete due to the periodic boundary condition, the actual trajectory has jumps and does not exactly coincide with the averaged path shown in Fig. 3. In fact, in between two jumps in the mode number, the value of E needs to increase at a larger rate than the average rate and the wave profile becomes broadened. At the jumps to the higher mode numbers, the value of E is suddenly reduced by a finite amount and the waves resume sharp profiles. These processes suggest that the energy is being built up in between the jumps and suddenly released at the jumps. On the return path into the metastable regime when the neutral pressure is reduced or the value of γ is increased [from (a) to (b)], we find that E decreases, but at a slightly smaller rate than that in the forward path in order to keep the same high mode number. Upon comparing the profiles of the ionized plasma for the stable low-m mode (c) and the metastable high-m mode (b) at the same neutral pressure, we find that the density contrast is significantly reduced for the metastable modes. Figure 2 also shows such a comparison. The metastable high-m mode (b) survives until the neutral pressure becomes so low that it must make a transition to a low-m mode; at this point, E decreases suddenly. Figure 3 plots the trajectory of the hysteresis described above in the (γ,E) parameter space.

To summarize, we have constructed a simple model, incorporating the ambipolar diffusion, wall losses, and ionization, to explain the nonlinear ionization wave patterns observed in experiments [7]. We consider the plasma dynamics

to be one-dimensional by properly taking into consideration the three-dimensional nature of the electric fields. It is found that this model contains an internally generated order parameter E. Even with the same experimentally controllable parameters, the ionization waves can assume different E's governed by some yet-to-be-understood mechanisms. This spontaneously generated order parameter E adds an extra degree of freedom to the system and makes it possible for the plasmas to exhibit hysteresis.

Of particular interest among the results of this work are the trajectories of hysteresis in the phase diagram. Hysteresis is known to be associated with the local minima in some form of energy landscapes. The unknown functions $G(E,\gamma)=C_a$ and $H(E,\gamma)=C_b$ shown in Fig. 3 are the expected trajectories of the local-energy minima, where $G=C_a$ traces the stable branch and $H=C_b$ traces the metastable branch. In the experiments [7], it was found that the system tends not only to follow the stable branches $G=C_a$ but also to follow the most stable branch that connects c and a, along which E assumes the minimally allowable value for a given γ.

However, in a two-dimensional phase space it is difficult to conceive how it is possible to support an energy landscape that has local minima on two continuous families of curves, unless the two families of curves are not continuous and C_a and C_b assume discrete values. The fact that the experiments always observe the plasma to follow the minimum-E curve of the stable family $G(E,\gamma)=C_a$ may have resulted from the discrete nature of C_a. It is only up to the future experiments which look into the details of the phase trajectories to test whether C_b also takes discrete values. If so, we expect that when the neutral gas is depressurized in the experiment, the trajectory along the stable family $G(E,\gamma)=C_a$ will first trace back along the original path; it is only at some specific discrete values of neutral pressure that the system can suddenly switch to the metastable state $H(E,\gamma)=C_b$. The origin of these expected discrete-energy minima should have little to do with the periodicity of the boundary, but reflect the genuine nature of the energy landscapes in the two-dimensional phase space. If this expected finding is confirmed by experiment, it will certainly reveal a new paradigm, with which one may gain deeper insights into the nature of hysteresis.

ACKNOWLEDGMENTS

We thank Lin I and T. M. Liu for helpful discussions regarding the experiments. This work was supported in part by the National Science Council of Taiwan under Grant Nos. NSC86-2112-M-008-018, NSC87-2112-M-008-009, and NSC87-2112-M-008-010. One of us (D.M.T.K.) gratefully acknowledges support from the National Science Council.

[1] D. B. Graves, IEEE Trans. Plasma Sci. **22**, 31 (1994).
[2] See, for example, *Protostars and Planets*, edited by E. H. Levy and J. I. Lunine (University of Arizona Press, Tucson, 1993) and *Meteorites and the Early Solar Systems*, edited by J. F. Kerridge and M. S. Matthews (University of Arizona Press, Tucson, 1988).
[3] Y. P. Raizer, M. N. Shneider, and N. A. Yatsenko, *Radio-Frequency Capacitance Discharges* (CRC Press, New York, 1995).
[4] J. H. Chu and Lin I, Phys. Rev. Lett. **72**, 4009 (1994).
[5] Y. Hayashi and K. Tachibana, J. Appl. Phys. **33**, L804 (1994).
[6] H. Thomas, G. E. Morfil, V. Demmel, J. Goree, B. Feuerbacher, and D. Mohlman, Phys. Rev. Lett. **73**, 652 (1994).
[7] J. B. Du, C. H. Chiang, and Lin I, Phys. Rev. E **54**, 1829 (1996).
[8] C. Y. Liu and Lin I, Phys Rev. E **57**, 3379 (1998).
[9] P. Kolodner, Phys. Rev. Lett. **69**, 2519 (1992).
[10] K. Krischer and A. Mikhailov, Phys. Rev. Lett. **75**, 3165 (1994).
[11] A. Ito and T. Ohta, Phys. Rev. A **45**, 8374 (1992).
[12] M. Tlidi, P. Mandel, and R. Lefever, Phys. Rev. Lett. **75**, 640 (1994).
[13] M. van Hecke, E. de Wit, and W. van Saarloos, Phys. Rev. Lett. **73**, 3930 (1995).
[14] R. J. Deissler and H. R. Brand, Phys. Rev. Lett. **74**, 4847 (1995).
[15] E. H. Rotermund, S. Kaubith, A. von Oertzen, and G. Ertl, Phys. Rev. Lett. **66**, 3083 (1991).
[16] F. F. Chen, *Introduction to Plasma Physics and Controlled Fusion* (Plenum, New York, 1983), p. 290.